Comp. Meth. Civil Eng., Vol. 3, 2 (2012) 47-66

CMCE
Computational Methods in Civil Engineering

Analysis of thin plates by a combination of isogeometric analysis and the Lagrange multiplier approach

N. Valizadeh[a], S.S. Ghorashi[b], S. Mohammadi[c*], S. Shojaee[a], H. Ghasemzadeh[b]

[a] *Department of Civil Engineering, University of Kerman, Kerman, Iran*
[b] *Department of Civil Engineering, K.N. Toosi University of Technology, Tehran, Iran*
[c] *School of Civil Engineering, University of Tehran, Tehran, Iran*

Received 16 February 2013; accepted in revised form 25 May 2013

Abstract

The isogeometric analysis is increasingly used in various engineering problems. It is based on Non-Uniform Rational B-Splines (NURBS) basis function applied for the solution field approximation and the geometry description. One of the major concerns with this method is finding an efficient approach to impose essential boundary conditions, especially for inhomogeneous boundaries. The main contribution of this study is to use the well-known Lagrange multiplier method to impose essential boundary conditions for improving the accuracy of the isogeometric solution. Moreover, Dirichlet boundary conditions on the derivatives of the solution field (which are not directly defined as independent degrees of freedom) can be treated easily. The Lagrange multipliers must be interpolated on a set of boundary points. Among the different available choices for the boundary interpolation points, the *Greville abscissas* are considered in this work. Several plate problems have been solved, which demonstrate significant improvement in accuracy and rate of convergence in comparison with the direct imposition of essential boundary conditions.

Keywords: Isogeometric analysis; NURBS; Essential boundary condition; Lagrange multiplier method; Kirchhoff plate; Greville abscissas.

1. Introduction

Isogeometric Analysis (IGA) has been developed [1] with the aim of integrating Non-Uniform Rational B-Splines (NURBS) based CAD into the finite element analysis. One of the main ideas in developing isogeometric analysis has been to prevent time-consuming data conversion between CAD systems and the finite element analysis (FEA) in engineering problems. IGA is based on Non-Uniform Rational B-Splines (NURBS) basis function applied for both the solution field approximation and the geometry description. Therefore, CAD and FEA can be unified efficiently in one package. This leads to the ability of modeling complex geometries accurately. Moreover, simple and systematic refinement strategies, exact representation of common engineering shapes, robustness and superior accuracy can be achieved in comparison with the conventional finite element method. Accordingly, the isogeometric analysis is expected to become a powerful computational approach in the

*Corresponding author.
Tel: +98-21-61112258, Fax: +98-21-66403808
E-mail address: smoham@ut.ac.ir

analysis of various engineering problems; as it has already been applied to structural problems, fluid mechanics, fluid-structure interaction, structural optimization, etc. [1-5]. In spite of important efforts dedicated to IGA, there are still many aspects that require further investigation. For instance, one of the key challenges with IGA is the imposition of essential boundary conditions. In isogeometric analysis, due to the non-interpolatory nature of NURBS basis functions, the kronecker-delta property is not satisfied. Therefore, similar to many meshfree methods such as EFG [6], RKPM [7] or SPH [8], imposition of essential boundary conditions in IGA is not a straightforward task. To impose the essential boundary conditions in numerical methods with non-interpolatory basis function, several strategies have been proposed [9]. These strategies can be classified into two categories [9]: 1) Methods based on a modified weak-form equation such as the Lagrange multiplier method [6], penalty method [10] and the Nitsche's method [11,12], 2) Methods based on a modified form of basis functions in order to reproduce the interpolation feature (see [13,14]). Embar et al. [15] employed the Nitsche's method to impose essential boundary conditions in spline based finite element method and second- and fourth-order boundary-value problems. They approximated the solution field using B-splines and the geometry was interpolated using bilinear Lagrangian shape functions for the interior elements and bicubic Lagrangian shape functions for the boundary elements. Nitsche's method is a variationally consistent and stabilized penalty method. One of the major disadvantages of this method is that the stability conditions for the system of equations must be set for each individual problem. Such stability parameters in the Nitsche's weak form are evaluated by solving a local generalized eigenvalue problem on the Dirichlet boundary. Wang et al. [16] improved the imposition of essential boundary condition in IGA using the transformation technique. In their proposed method, a relation between control variables (degrees of freedom defined on control points) and the collocated nodal values at the essential boundary is obtained. By using open knot vectors in the transformation method, the NURBS basis functions corresponding to interior control points vanish at the boundaries and the control points can be simply separated to interior control points and boundary ones. Therefore, the approximation of solution field variable can be expressed as a combination of interior and boundary control variables. Then, by collocation of solution field variable in a set of boundary nodes, the boundary control variables can be purely related to their physical values at the essential boundary. Costantini et al. [17] applied the quasi-interpolation method to impose Dirichlet boundary conditions in isogeomtric analysis based on generalized B-splines, avoiding interpolation of inhomogeneous essential boundary data in the approximation space which was a global approach and required solving a linear system of equations. The quasi-interpolation technique is a local approach and while it does not require solution of large "global" linear systems, it provides the same level of accuracy [17-25].

Since the Lagrange multiplier method is straightforward to implement and does not need separation of interior and boundary control points [9] and based on a similar approach for 2D continuum problems [26], it has been selected for improving the imposition of essential boundary conditions in IGA analysis of plates.

This paper is organized as follows. In Section 2, the NURBS basis function is briefly reviewed. In addition, a general formulation of NURBS-based isogeometric analysis is presented. Then, imposition of essential boundary conditions in the isogeometric analysis using the Lagrange multiplier method is discussed in Section 3. In Section 4, results of the numerical simulations of several problems are discussed and the efficiency of the proposed approach is assessed by comparing with available reference results.

2. NURBS-based isogeometric analysis

The concept of isogeometric analysis, which has been recently proposed by Hughes et al. [1], is to apply the same basis functions which are used to accurately describe the geometry for the approximation of the physical variables. Since NURBS basis functions have become the standard basis for describing and modeling the geometry in CAD and computer graphics, they are used for describing both the geometry and the solution space.

2.1 NURBS basis function

NURBS are a generalization of piecewise polynomial B-spline curves. The B-spline basis functions are defined in a parametric space on a knot vector Ξ. A knot vector in one dimension is a non-decreasing sequence of real numbers:

$$\Xi = \left\{\xi_1, \xi_2, ..., \xi_{n+p+1}\right\} \tag{1}$$

where ξ_i is the i^{th} knot, i is the knot index, $i = 1, 2, ..., n+p+1$, p is the order of the B-spline, and n is the number of basis functions. The half open interval $\left[\xi_i, \xi_{i+1}\right)$ is called the i^{th} knot span and it can have zero length since knots may be repeated more than once, and the interval $\left[\xi_1, \xi_{n+p+1}\right]$ is called a patch. In the isogeometric analysis, always open knot vectors are employed. A knot vector is said to be open if it has $p+1$ repeating knots at the two ends.

With a certain knot span, the B-spline basis functions are defined recursively as,

$$N_{i,0}(\xi) = \begin{cases} 1 & \text{if } \xi_i \le \xi \le \xi_{i+1} \\ 0 & \text{otherwise} \end{cases} \tag{2}$$

and

$$N_{i,p}(\xi) = \frac{\xi - \xi_i}{\xi_{i+p} - \xi_i} N_{i,p-1}(\xi) + \frac{\xi_{i+p+1} - \xi}{\xi_{i+p+1} - \xi_{i+1}} N_{i+1,p-1}(\xi), \quad p = 1,\ 2,\ 3,\ \ldots\ . \tag{3}$$

where $i = 1, 2, ..., n$.

A B-spline curve of order p is defined by:

$$C(\xi) = \sum_{i=1}^{n} N_{i,p}(\xi) P_i. \tag{4}$$

where $N_{i,p}(\xi)$ is the i^{th} B-spline basis function of order p and P are control points, given in d-dimensional space $\mathbf{R}^d$. 1-D B-splines basis functions which are built from open knot vectors, are interpolatory at the ends of parametric space. Figure 1 shows the quadratic B-spline basis functions with the interpolation feature at the ends of parametric space. In two dimensions, B-spline basis functions become interpolatory at the corners of the patches.

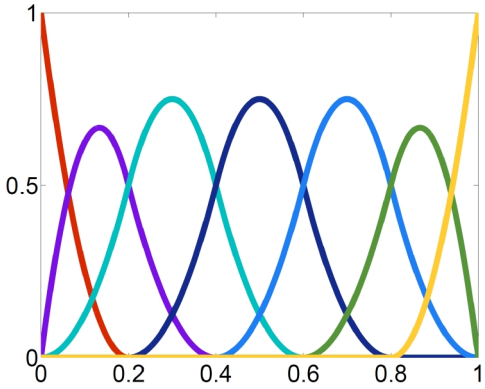

Figure 1. Quadratic basis functions for an open knot vector $\Xi = \{0,0,0,0.2,0.4,0.6,0.8,1,1,1\}$.

The non-uniform rational B-spline (NURBS) curve of order p is defined as:

$$C(\xi) = \sum_{i=1}^{n} R_{i,p}(\xi) P_i \tag{5}$$

$$R_{i,p}(\xi) = \frac{N_{i,p}(\xi) w_i}{\sum_{i=1}^{n} N_{i,p}(\xi) w_i} \tag{6}$$

Here $R_{i,p}$ is the NURBS basis function, P_i is the control point and w_i is the i^{th} weight that must be non-negative. In the two dimensional parametric space $[0,1]^2$, NURBS surfaces are constructed by tensor product through knot vectors $\Xi = \{\xi_1, \xi_2, ..., \xi_{n+p+1}\}$ and $\mathrm{H} = \{\eta_1, \eta_2, ..., \eta_{m+q+1}\}$. It yields to:

$$S(\xi,\eta) = \sum_{i=1}^{n} \sum_{j=1}^{m} R_{i,j}^{p,q}(\xi,\eta) P_{i,j} \tag{7}$$

where $P_{i,j}$ is the (i,j)-th of $n \times m$ control points, also called the control mesh. The interval $[\xi_1, \xi_{n+p+1}] \times [\eta_1, \eta_{m+q+1}]$ is a patch and $[\xi_i, \xi_{i+1}) \times [\eta_j, \eta_{j+1})$ is a knot span. $R_{i,j}^{p,q}(\xi,\eta)$ is the NURBS basis function in two dimensional space,

$$R_{i,j}^{p,q}(\xi,\eta) = \frac{N_{i,p}(\xi) M_{j,q}(\eta) w_{i,j}}{W_{i,j}(\xi,\eta)} \tag{8}$$

and

$$W_{i,j}(\xi,\eta) = \sum_{i=1}^{n} \sum_{j=1}^{m} N_{i,p}(\xi) M_{j,q}(\eta) w_{i,j} \tag{9}$$

The derivative of $R_{i,j}^{p,q}(\xi,\eta)$ with respect to ξ is derived by simply applying the quotient rule to (8):

$$\frac{\partial R_{i,j}^{p,q}(\xi,\eta)}{\partial \xi} = \frac{N'_{i,p}(\xi) M_{j,q}(\eta) w_{i,j} W_{i,j}(\xi,\eta) - \frac{\partial W_{i,j}(\xi,\eta)}{\partial \xi} N_{i,p}(\xi) M_{j,q}(\eta) w_{i,j}}{(W_{i,j}(\xi,\eta))^2} \tag{10}$$

and

$$\frac{\partial W_{i,j}(\xi,\eta)}{\partial \xi} = \sum_{i=1}^{n}\sum_{j=1}^{m} N'_{i,p}(\xi) M_{j,q}(\eta) w_{i,j} \tag{11}$$

The domain of problem is divided into patches and each patch is divided into knot spans or elements. Patches play the role of sub-domains within which element types and material models are assumed to be uniform [1]. Nevertheless, many complicated domains can be represented by a single patch.

For more details on NURBS, refer to [18].

2.2 NURBS based isogeometric analysis formulation

In an isogeometric approach, the discretization is based on NURBS basis functions. Geometry and solution fields are approximated as,

$$\mathbf{x}(\xi,\eta) = \sum_{i=1}^{n_{en}} R_i(\xi,\eta) \begin{Bmatrix} P_i^x \\ P_i^y \end{Bmatrix} = \sum_{i=1}^{n_{en}} R_i(\xi,\eta)\mathbf{P}_i \tag{12}$$

$$\mathbf{u}^h(\xi,\eta) = \sum_{i=1}^{n_{en}} R_i(\xi,\eta)\mathbf{u}_i \tag{13}$$

where $0 \le \xi,\eta \le 1$ and $\mathbf{x} = \{x \quad y\}^T$. $n_{en} = (p+1)\times(q+1)$ is the number of nonzero basis basis functions for a given knot span (element). R_i and $\mathbf{P}_i = \{P_i^x \quad P_i^y\}^T$ are the i -th NURBS basis function and control point, respectively.

$\mathbf{u}_i$ is the i -th solution field value at the control points, which are also called a control variable.

2.2.1 Kirchhoff plates

Plates are geometrically similar to 2D solids with the difference that forces are applied perpendicular to the plane of plate (see Figure 2). Therefore, a plate experiences bending and deflection w in the z direction; both function of position x and y . The stress σ_{zz} in a plate is assumed to be zero. The Kirchhoff plate theory, also called the classic plate theory (CPT), assumes that normals to the neutral surface of the undeformed plate remain straight and normal to the neutral surface during the deformation/bending.

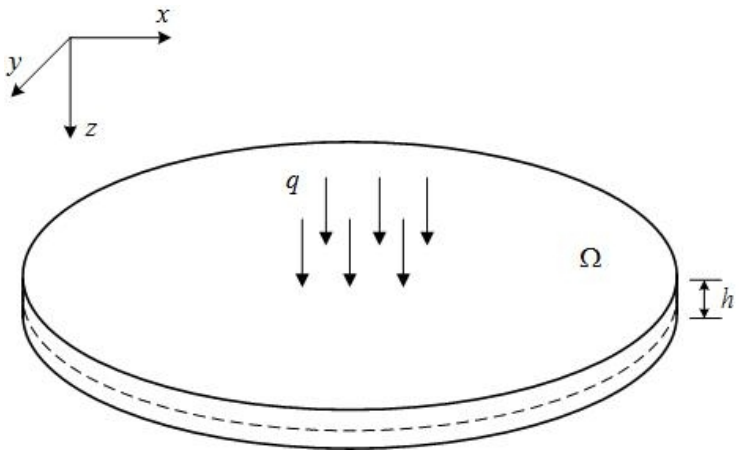

Figure 2. Plate subjected to transverse loading.

The strong form of governing equation for a CPT problem and corresponding boundary conditions can be written as

$$\nabla^4 w = \frac{q}{D_0} \quad \text{in } \Omega \tag{14}$$

$$\boldsymbol{\sigma}\mathbf{n} = \bar{\mathbf{t}} \quad \text{on } \Gamma_t \tag{15}$$

$$\tilde{\mathbf{w}} = \bar{\mathbf{w}} \quad \text{on } \Gamma_u \tag{16}$$

where Ω denotes the domain of the problem, w is the deflection of the plate and q is uniform load. $D_0 = \dfrac{Eh^3}{12(1-\nu^2)}$ is the bending stiffness of the plate, where E, h and ν are the Young's modulus, plate thickness and Poisson's ratio, respectively. $\bar{\mathbf{t}}$ is the prescribed boundary forces on the natural boundary and $\bar{\mathbf{w}}$ is the prescribed displacement on the essential boundary.

In equation (16), $\tilde{\mathbf{w}}$ is a vector defined as $\tilde{\mathbf{w}} = \mathbf{Q}w$, where $\mathbf{Q}$ is defined as $\left\{1 \quad \dfrac{\partial^2}{\partial n^2}\right\}^T$ and $\mathbf{Q} = \left\{1 \quad \dfrac{\partial}{\partial n}\right\}^T$ for simply supported and clamped boundaries, respectively.

The weak form of equation (14) can be written as,

$$\int_\Omega \delta\boldsymbol{\varepsilon}_p^T \boldsymbol{\sigma}_p d\Omega - \int_\Omega \delta w q d\Omega - \int_{\Gamma_t} \delta\mathbf{u}^T \bar{\mathbf{t}} d\Gamma = 0 \tag{17}$$

where $\boldsymbol{\varepsilon}_p$ and $\boldsymbol{\sigma}_p$ are the pseudo-strain and the pseudo-stress vectors, respectively and $\mathbf{u}$ is the displacement field of the Kirchhoff plate [19],

$$\mathbf{u} = \begin{Bmatrix} u \\ v \\ w \end{Bmatrix} = \left\{ -z\frac{\partial}{\partial x} \quad -z\frac{\partial}{\partial y} \quad 1 \right\}^T w = \mathbf{L}_u w \tag{18}$$

The pseudo-strain and pseudo-stress (per unit length) are defined as,

$$\boldsymbol{\varepsilon}_p = \left\{ -\frac{\partial^2}{\partial x^2} \quad -\frac{\partial^2}{\partial y^2} \quad -2\frac{\partial^2}{\partial x \partial y} \right\}^T w = \mathbf{L}w \tag{19}$$

$$\boldsymbol{\sigma}_p = \left\{ M_x \quad M_y \quad M_{xy} \right\}^T = D_0 \mathbf{D} \boldsymbol{\varepsilon}_p \tag{20}$$

where

$$\mathbf{D} = \begin{bmatrix} 1 & \nu & 0 \\ \nu & 1 & 0 \\ 0 & 0 & \dfrac{1-\nu}{2} \end{bmatrix} \tag{21}$$

The solution field (deflection) can be approximated by equation (13):

$$w^h(\xi,\eta) = \sum_{i=1}^{n_{en}} R_i(\xi,\eta) w_i \tag{22}$$

where w_i is i -th component of the vector of control variables $\mathbf{w}$ obtained by solving the following discretized equilibrium equation,

$$\mathbf{Kw} = \mathbf{f} \tag{23}$$

The stiffness matrix $\mathbf{K}$ and the force vector $\mathbf{f}$ are given in equations (24) and (25), respectively.

$$\mathbf{K}_{ij} = \int_{\Omega} \mathbf{B}_i^T D_0 \mathbf{D} \mathbf{B}_j d\Omega \tag{24}$$

$$\mathbf{f}_i = \int_{\Omega} R_i q d\Omega + \int_{\Gamma_t} \mathbf{F}_i^T \overline{\mathbf{t}} d\Gamma \tag{25}$$

where

$$\mathbf{B}_i = \begin{Bmatrix} -R_{i,xx} \\ -R_{i,yy} \\ -2R_{i,xy} \end{Bmatrix}, \quad \mathbf{F}_i = \begin{Bmatrix} -zR_{i,x} \\ -zR_{i,y} \\ R_i \end{Bmatrix} \tag{26}$$

3. Imposing essential boundary conditions using the Lagrange multiplier method

Imposing essential boundary conditions in numerical methods that do not possess the Kronecker delta property is not usually straightforward. Since an isogeometric analysis uses NURBS basis functions that do not satisfy the Kronecker delta property, this method suffers from this drawback. It is well worth noting that direct imposition of homogeneous essential boundary conditions to the control variables, as discussed in [1], has no difficulty, but imposing inhomogeneous essential boundary conditions needs new developments [1].

It should be noted that the present isogeometric formulation based on Kirchhoff plate theory is rotation-free. In other words, only the deflections of the plate are degrees of freedom and rotations can be calculated as derivatives of deflection but are not degrees of freedom [1]. Therefore, rotational boundary conditions need to be imposed by an appropriate approach.

For these reasons, the Lagrange multiplier method is employed in this study as a scheme for treatment of essential boundary conditions.

3.1 Kirchhoff plates

Similar procedure is utilized for adopting the Lagrange multiplier method in analyzing thin plates. The essential boundary condition (equation (16)) is converted into the following integral form using the Lagrange multiplier $\boldsymbol{\lambda}$:

$$\int_{\Gamma_u} \boldsymbol{\lambda}^T (\tilde{\mathbf{w}} - \overline{\mathbf{w}}) d\Gamma \tag{27}$$

As a result, two additional boundary condition terms are added to the weak form of the static elastic equilibrium equation of thin plates. This modified weak form can be written as

$$\int_{\Omega} \delta \boldsymbol{\varepsilon}_p^T \boldsymbol{\sigma}_p d\Omega - \int_{\Omega} \delta w q d\Omega - \int_{\Gamma_t} \delta \mathbf{u}^T \overline{\mathbf{t}} d\Gamma - \int_{\Gamma_u} \delta \boldsymbol{\lambda}^T (\tilde{\mathbf{w}} - \overline{\mathbf{w}}) d\Gamma - \int_{\Gamma_u} \delta \tilde{\mathbf{w}}^T \boldsymbol{\lambda} d\Gamma = 0 \tag{28}$$

To obtain the discretized equation from this weak form, the Lagrange multipliers must be discretized. As discussed in [9], among several possibilities for the choice of the interpolation space for the Lagrange multiplier, the NURBS and Lagrange shape functions can be chosen. In this study, Lagrange multipliers are interpolated on essential boundary using the Lagrange shape functions. The Lagrange multipliers are defined at several essential boundary points.

An appropriate choice for these desired essential boundary points is the *Greville abscissas* [20], defined as,

$$g_i^p = \frac{\xi_{i+1} + ... + \xi_{i+p}}{p}, \qquad i = 1, ..., n \tag{29}$$

where p is the NURBS order and n is the number of control points.

If the number of Lagrange multipliers is too large, the resulting system of equations can be ill-conditioned, whereas for very small number of Lagrange multipliers, the essential boundary condition cannot be imposed accurately. In fact, the interpolation space for Lagrange multipliers and for the solution field variable must satisfy an inf-sup condition, known as the Babuska-Brezzi stability condition [21,22], in order to ensure the convergence of approximation [9].

Interpolating the Lagrange multipliers using 1D Lagrange shape functions on physical boundary points corresponding to Greville abscissas, leads to

$$\lambda(u) = \sum_{i=1}^{n_\lambda} S_i(u)\, \lambda_i \tag{30}$$

where $S_i(u)$ is the 1D Lagrange basis function and n_λ is the number of the essential boundary points applied for this interpolation.

Substituting the deflection of the plate w from (22) into the weak form (28) leads to the following discretized equations:

$$\begin{pmatrix} \mathbf{K} & \mathbf{G} \\ \mathbf{G}^T & \mathbf{0} \end{pmatrix} \begin{pmatrix} \mathbf{w} \\ \boldsymbol{\lambda} \end{pmatrix} = \begin{pmatrix} \mathbf{f} \\ \mathbf{q} \end{pmatrix} \tag{31}$$

$\mathbf{K}$ and $\mathbf{f}$ are the same as those defined in Eqs. (24) and (25), respectively. The nodal matrix $\mathbf{G}_{ij}$ and the vector $\mathbf{q}_i$ are defined as,

$$\mathbf{G}_{ij} = -\int_{\Gamma_u} \mathbf{S}_i(u) \boldsymbol{\Psi}_j(\xi, \eta) d\Gamma \tag{32}$$

$$\mathbf{q}_i = -\int_{\Gamma_u} \mathbf{S}_i(u) \bar{\mathbf{w}} d\Gamma \tag{33}$$

where

$$\mathbf{S}_i = \begin{bmatrix} S_i & 0 \\ 0 & S_i \end{bmatrix} \tag{34}$$

$$\boldsymbol{\Psi}_j(\xi, \eta) = \begin{bmatrix} R_j(\xi, \eta) \\ R_{j,n}(\xi, \eta) \end{bmatrix} \quad \text{For a clamped boundary}$$

$$\boldsymbol{\Psi}_j(\xi, \eta) = \begin{bmatrix} R_j(\xi, \eta) \\ R_{j,nn}(\xi, \eta) \end{bmatrix} \quad \text{For a simply supported boundary} \tag{35}$$

S_i is defined in (3) and n is the unit normal to the essential boundary Γ_u.

4. Numerical simulations

In this section, several numerical problems are solved to illustrate the superior accuracy and acceptable rate of convergence of the proposed approach in comparison with the direct imposition of essential boundary conditions on control variables. In this study, direct imposition of essential boundary conditions on the control variables, means that the function of essential boundary condition is evaluated on the physical position of boundary control points and the obtained values are assigned to the corresponding control variables. In all examples, the number of Gauss points in each direction is considered $\max(p+1, 4)$, where

p is the order of NURBS basis function. For the convergence study, h-refinement strategy has been applied to the initial geometry of model. In each refinement step, knots are added to the middle of knot spans.

First a number of rather simple 2D continuum problems are solved to evaluate the performance of the Lagrange/IGA approach and then several bending problems are simulated.

4.1 Laplace problem on a square domain

For the first example, the Laplace problem is solved on a unit square domain:

$$\begin{cases} \nabla^2 u = 0 \\ u(x,0) = \sin(\pi x) \qquad\qquad \mathbf{x} \in [0,1]^2 \\ u(x,1) = u(0,y) = u(1,y) = 0 \end{cases} \tag{36}$$

where ∇^2 denotes the Laplacian operator. The analytical solution for this problem is:

$$u^{ex}(x,y) = [\cosh(\pi y) - \coth(\pi)\sinh(\pi y)]\sin(\pi x) \tag{37}$$

The geometry is constructed by a NURBS surface of order $p = 3$ for both directions with unit weights. Initial discretized geometry is shown in Figure 3. The initial knot vectors in the parametric space are $\{0,0,0,0,0.5,1,1,1,1\}$. To study the convergence of the numerical approach, h-refinement strategy is employed and meshes with 16, 64, 256 and 1024 elements are investigated (see Figure 4). The isogeometric solution and the absolute error for the Lagrange multiplier method on a model with 256 elements are plotted in Figure 5. Results of L^2 and H^1 error norms are shown in Figures 6 and 7 in terms of the maximum knot span dimension h. As expected, a quartic convergence rate for the L^2 error norm and a cubic rate of convergence for the H^1 error norm have been obtained by the Lagrange multiplier method, which are comparable with the quadratic rate in both cases for the direct imposition of boundary conditions; showing the superior accuracy and optimal rate of convergence of the present approach. This problem was also solved by Embar et al. [15] with the Nitsche's method and spline-based finite elements. As shown in Figures 6 and 7, the present Lagrange multiplier method provides more or less the same level of accuracy and the convergence rate as the Nitsche's approach.

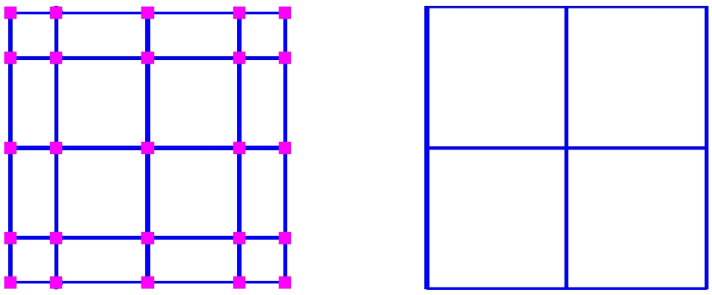

Figure 3. Initial discretized geometry: (left) control mesh; (right) physical mesh

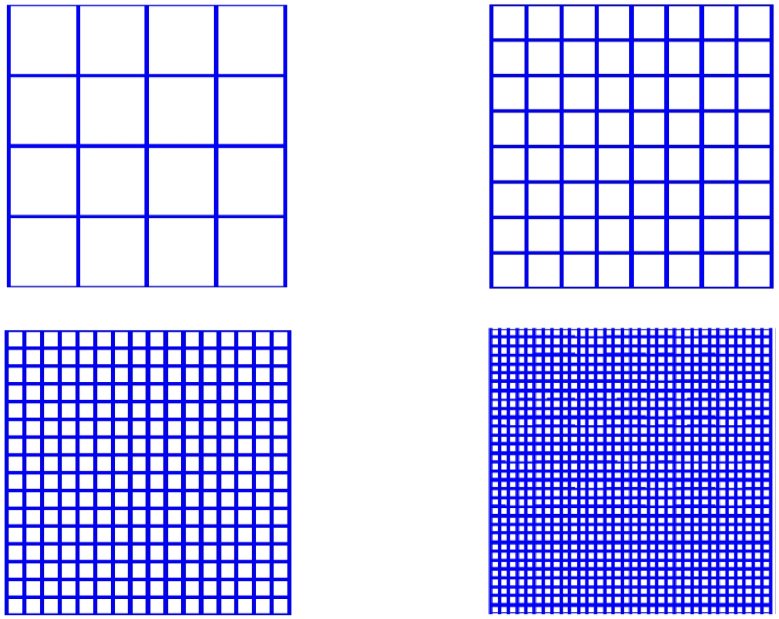

Figure 4. Physical meshes with 16, 64, 256 and 1024 elements for the convergence study

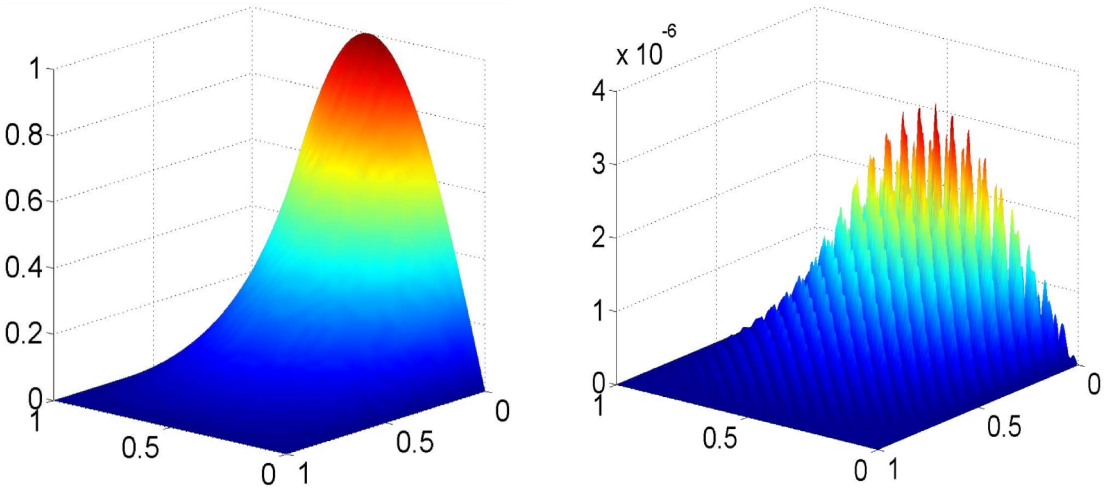

Figure 5. Isogeometric solution with 256 elements (Left) and absolute error (Right) based on the Lagrange multiplier method

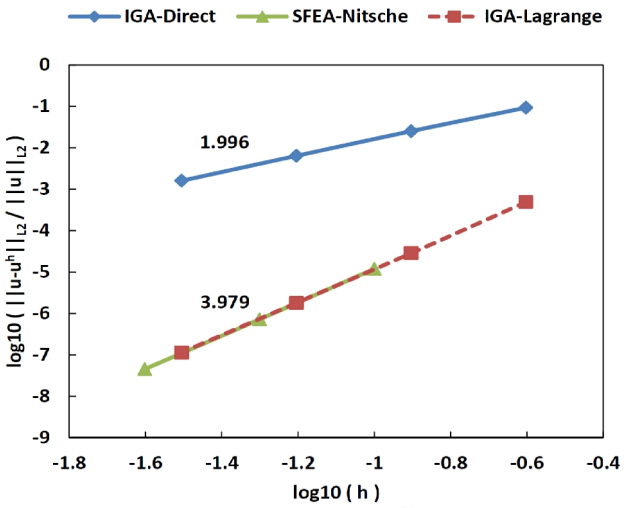

Figure 6. Comparison of L^2 error norm

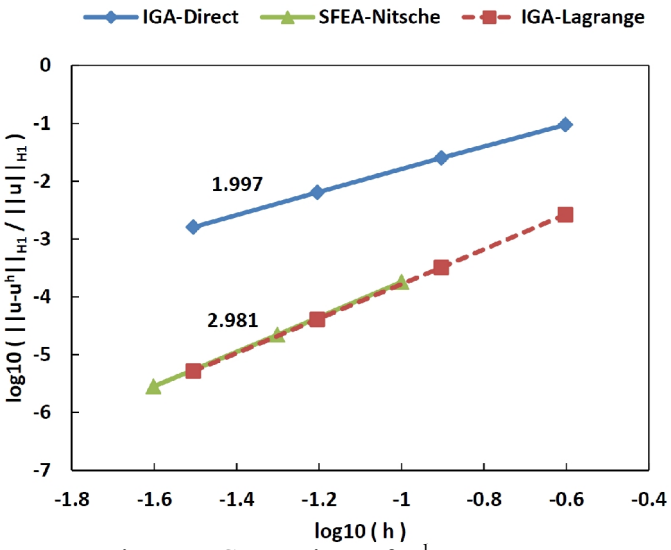

Figure 7. Comparison of H^1 error norm

4.2 Potential problem on a quarter of an annulus

Consider a potential problem on a quarter of an annulus (Figure 8). The governing equation and boundary conditions are given as follows:

$$\begin{cases} \nabla^2 u + s = 0 \text{ in } \Omega \\ n.\nabla u = \overline{t} \quad \text{on } \Gamma_t \\ u = \overline{u} \quad \text{on } \Gamma_u \end{cases} \tag{38}$$

Where s is the source term. This problem has been also studied by Costantini et al. [17] for B-spline and generalized B-spline basis functions. The exact solution for this problem is obtained as,

$$u(x,y) = \sin((x^2 + y^2 - 1)/5) \tag{39}$$

Prescribed Dirichlet boundary conditions are calculated from the exact solution and imposed on all the boundaries of the domain. In this problem, no traction is considered. The source term s can also be derived from the exact solution (39). In order to compare with the quasi-interpolation method [17], the initial geometry is constructed by tensor product of quadratic NURBS basis functions, as shown in Figure 9. The initial parametric space is given by two knot vectors of the same form: $\{0,0,0,0.5,1,1,1\}$. Using the h-refinement strategy, meshes with 4, 16, 64, 256 and 1024 elements are considered for the convergence study (see Figure 10). The isogeometric solution with 256 elements and based on the Lagrange multiplier method is depicted in Figure 11. The absolute error distribution is also plotted in Figure 11. The discrete L^2 error norm, computed on a 100×100 grid, is presented in Table. 1 and Figure 12 and compared with the results of quasi-interpolation and direct methods. It can be clearly observed from Figure 12 that the Lagrange multiplier method presents superior accuracy and higher rate of convergence in comparison with the direct method. Also the results of proposed approach are slightly better than those obtained by the quasi-interpolation method.

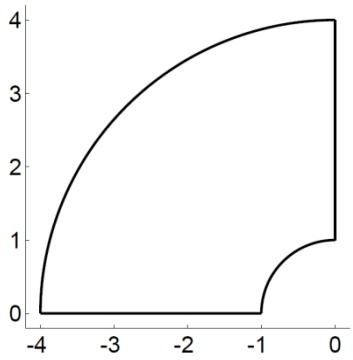

Figure 8. Potential problem on a quarter of an annulus

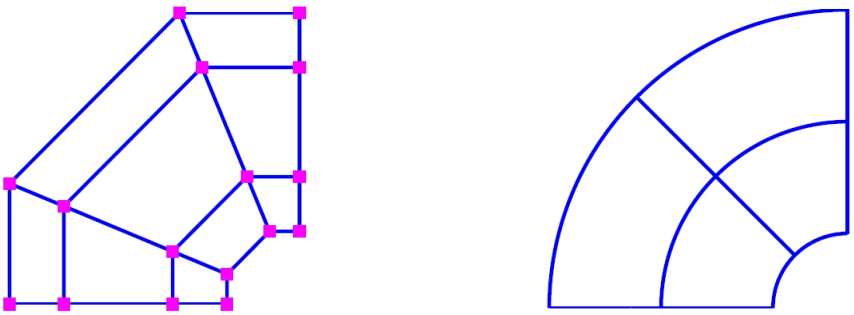

(a) (b)

Figure 9. Initial geometry model: (a) control mesh; (b) physical mesh (elements)

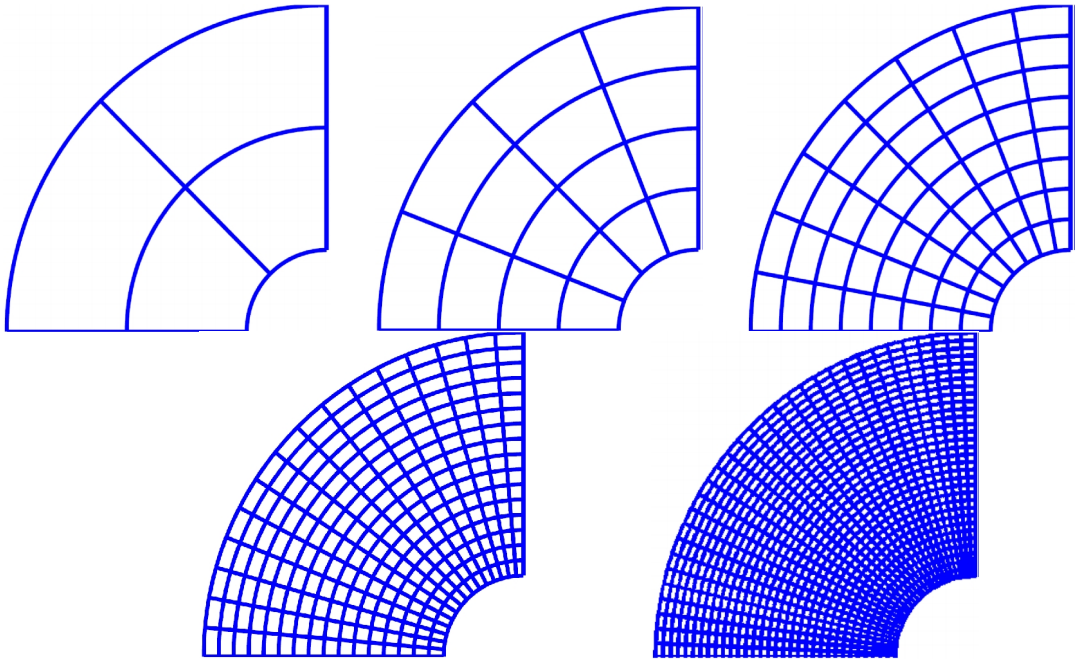

Figure 10. Physical meshes with 4, 16, 64, 256 and 1024 elements used for convergence study

Table 1. Comparison of discrete L^2 error norm

Num. of elements per side	IGA-Direct	IGA-Lagrange	IGA-Quasi interpolation [17]
2	23.910E+00	1.1890E+00	2.8273E+00
4	7.0331E+00	4.9354E-01	5.7032E−01
8	1.8218E+00	4.7802E-02	5.3653E−02
16	4.6078E-01	5.2440E-03	5.5270E−03
32	1.1563E-01	6.1690E-04	6.3060E−04

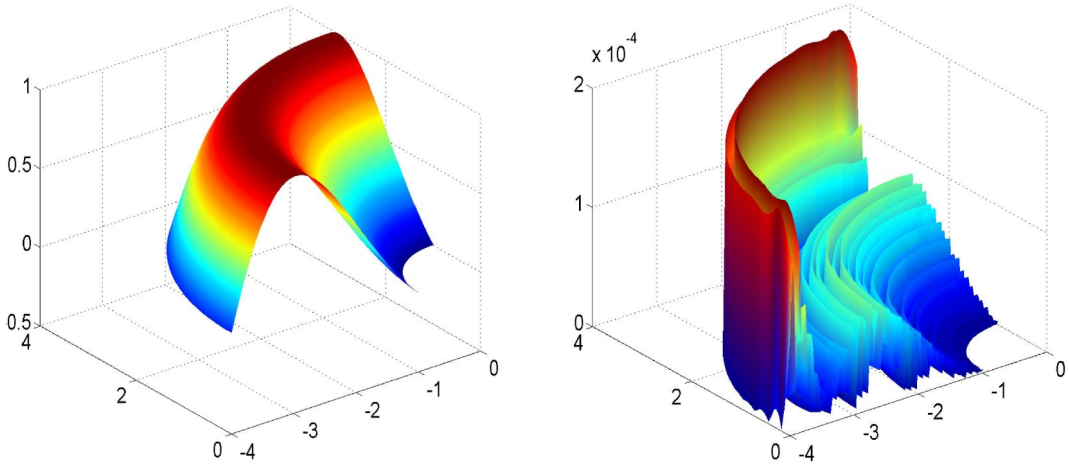

Figure 11. Isogeometric solution (Left) and absolute error (Right) on a model of 256 elements based on the Lagrange multiplier method

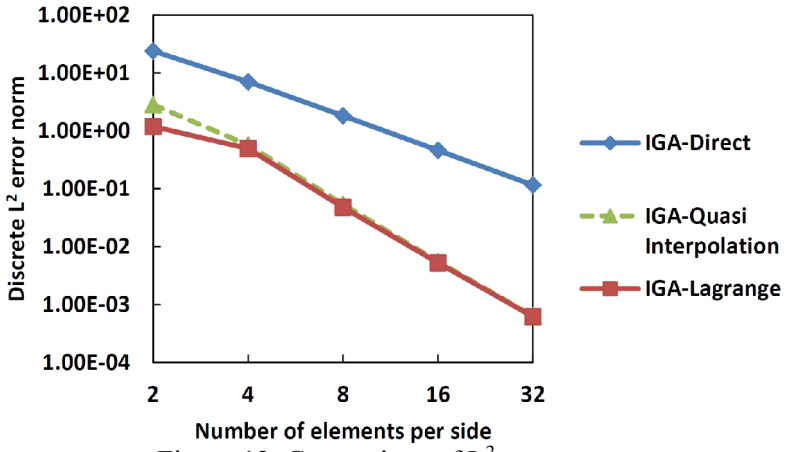

Figure 12. Comparison of L^2 error norm

4.3 An infinite plate with a central circular hole

The third example is a plane stress infinite tensile plate with a central circular hole, as depicted in Figure 13. Geometric and mechanical parameters are assumed as: radius of the circular hole $R=1$, plate width $L=4$, Young's modulus $E=10^5$, Poisson's ratio $\nu=0.3$ and traction $T_x=10$,.

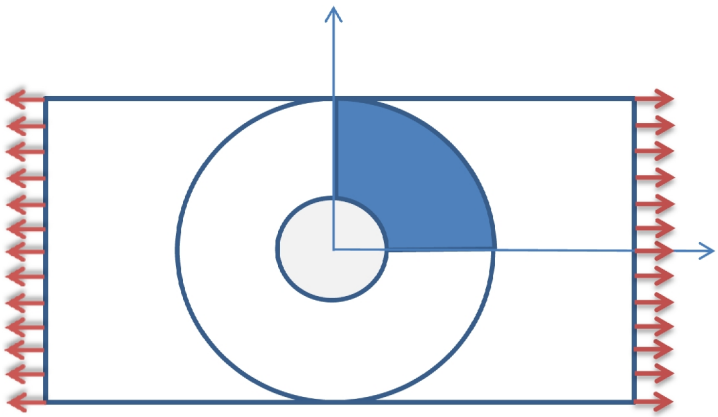

Figure 13. Infinite plate with a central circular hole

Only one quarter of a circular finite domain of the problem is simulated (see Figure 13). In order to represent the infinite plate, the analytical displacements are imposed as the essential boundary conditions on the boundary of the circular domain: [23]

$$u_x(r,\theta)=\frac{T_x R}{8\mu}\left[\frac{4r}{R(1+\nu)}\cos\theta+\frac{2R}{r}\left(\frac{4\cos\theta}{1+\nu}+\cos 3\theta\right)-\frac{2R^3}{r^3}\cos 3\theta\right] \tag{40}$$

$$u_y(r,\theta)=\frac{T_x R}{8\mu}\left[\frac{-4r\nu}{R(1+\nu)}\sin\theta+\frac{2R}{r}\left(\frac{-2(1-\nu)\sin\theta}{1+\nu}+\sin 3\theta\right)-\frac{2R^3}{r^3}\sin 3\theta\right] \tag{41}$$

where μ is the shear modulus.

Two knot vectors of the same form $\{0,0,0,1,1,1\}$ are used to define the initial parametric space. Meshes with 4, 16, 64, 256 and 1024 elements are considered for the convergence study (see Figure 14). The L^2 and H^1 error norms are plotted in Figures 15 and 16, which show that near cubic and quadratic convergence rates for the L^2 and H^1 error norms are obtained for the Lagrange multiplier method. In addition, higher solution accuracy is obtained by the present method.

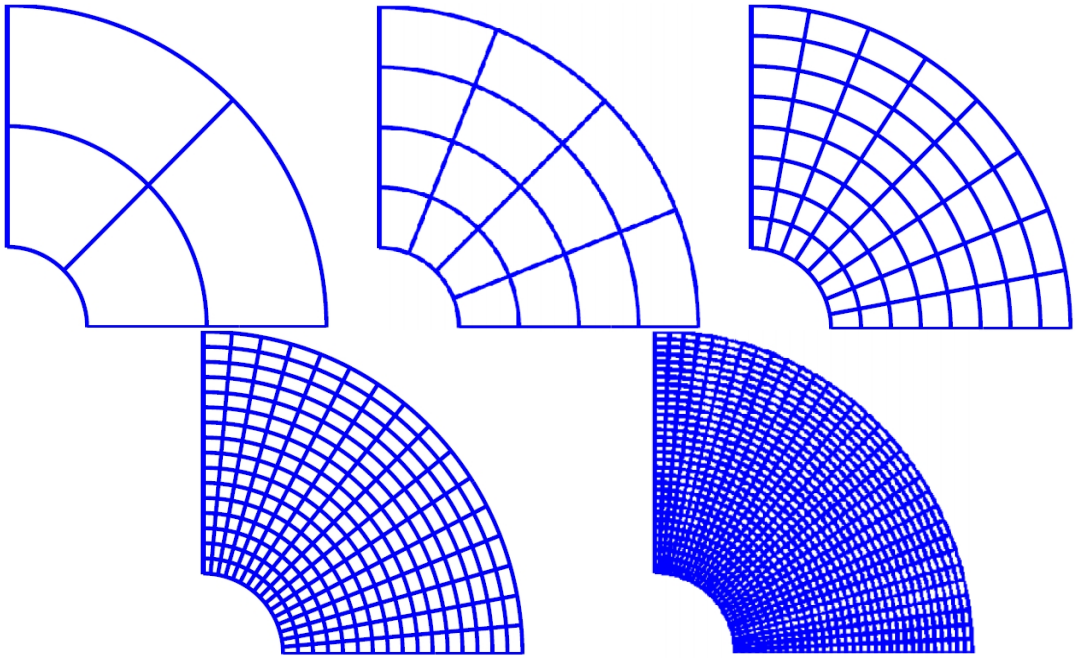

Figure 14. Physical meshes with 4, 16, 64, 256 and 1024 elements

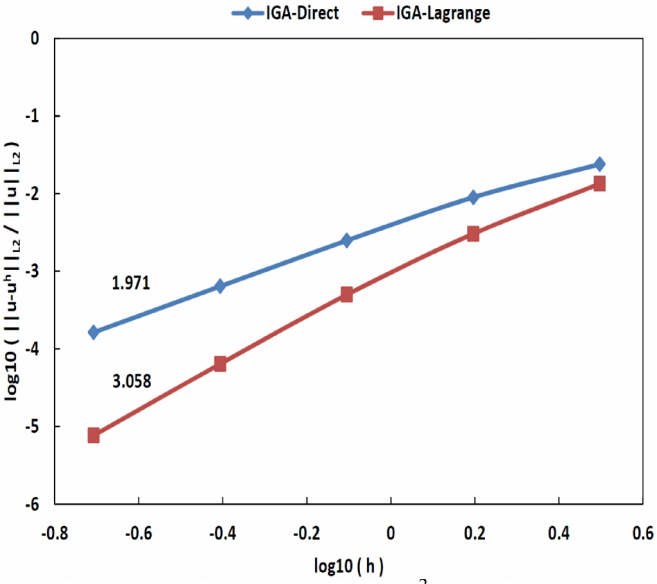

Figure 15. Comparison of L^2 error norm

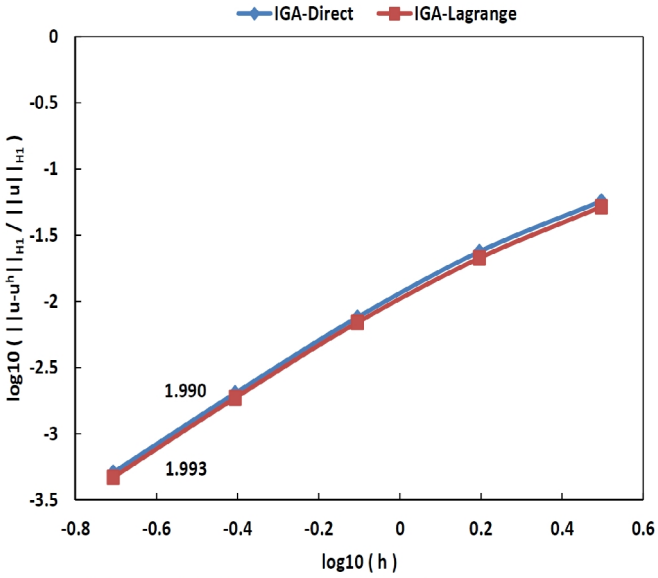

Figure 16. Comparison of H^1 error norm

4.4 Static bending analysis of rectangular thin plates

In this example, application of Lagrange multiplier method in isogeometric analysis is investigated for thin plate problems which boundary conditions are defined on both the solution field and its first or second derivative (see Sec. 3.1). For this purpose, a thin plate under a concentrated load is modeled with different boundary conditions: (SSSS) simply supported boundary conditions on all sides, and (CCCC) clamped boundary conditions on all sides. The following parameters are assumed: Length of the plate in x-direction $L_x = 0.6\,m$ for rectangular plates, $L_x = L_y = 0.6\,m$ for square plates, $h = 0.001\,m$ plate thickness, $E = 10^9\,N/m^2$ Young's modulus, $\nu = 0.3$ Poisson's ratio. The concentrated load $P = 100\,N$ is applied at the center of the plate. The center deflection of the plate $w_{\max}$ is calculated and normalized using the following coefficient $\bar{w} = \dfrac{w_{\max} D_0}{P L_x^2}$.

Cubic order NURBS basis functions with 16, 64, 256 and 1024 elements have been investigated and the results for a square plate with simply supported and clamped boundary conditions are shown in Table 2. It can be seen that the results of the proposed method quickly converge to the analytical solution.

Tables 3 and 4 present the results of the proposed method with different width/length ratios for (SSSS) and (CCCC) boundary conditions, respectively. These results are obtained by cubic NURBS basis function with 64 elements and 121 control points. Again, a good agreement between IGA and analytical solution can be found.

Table 2. Dimensionless central deflection of square plate under concentrated load

	Present Method (IGA)				Analytical Solution [24]
Number of Elements	4×4	8×8	16×16	32×32	
SSSS	0.0114	0.0116	0.0116	0.0116	0.0116
CCCC	0.0054	0.0056	0.0056	0.0056	0.0056

Table 3. Dimensionless central deflection of rectangular plates with different aspect ratios under concentrated load for simply supported boundary condition (p=q=3, 64 elements, 121 control points)

L_y/L_x	1.0	1.2	1.4	1.6	1.8	2.0
$\bar{w}$ (IGA)	0.0116	0.0135	0.0148	0.0156	0.0161	0.0164
$\bar{w}$ (Analytical Solution)	0.0116	0.0135	0.0148	0.0157	0.0162	0.0165

Table 4. Dimensionless central deflection of rectangular plates with different aspect ratios under concentrated load for clamped boundary condition (p=q=3, 64 elements, 121 control points)

L_y/L_x	1.0	1.2	1.4	1.6	1.8	2.0
$\bar{w}$ (IGA)	0.0056	0.0064	0.0069	0.0070	0.0071	0.0071
$\bar{w}$ (Analytical Solution)	0.0056	0.0065	0.0069	0.0071	0.0072	0.0072

4.5 Elliptical plate under uniform load

As the last example, a fully clamped elliptical plate subjected to a uniform load is investigated. In this problem, Dirichlet boundary conditions are defined on both the solution field and its first derivative. The radii of the elliptical plate are a = 5 m and b = 2.5 m, respectively. Other parameters are assumed as: plate thickness $h = 0.001m$, Young's modulus $E = 10^9 N/m^2$, Poisson's ratio $\nu = 0.3$, and the uniform load $q = 100N$. The deflection of the plate computed by IGA is normalized using the following coefficient $\bar{w} = \frac{8wD_0}{q}$. There is an exact solution for this problem which is obtained by the following formula [25]:

$$w = \frac{q}{8D_0}\frac{a^4b^4(x^2/a^2 + y^2/b^2 - 1)^2}{3a^4 + 3b^4 + 2a^2b^2} \tag{42}$$

where q is the uniform load.

To model the geometry of this example, we use a very coarse mesh as the initial geometry which is constructed by a NURBS surface of order $p = 2$ in both directions. This initial discretized geometry is shown in Figure 17. The initial knot vectors in the parametric space

are $\{0,0,0,1,1,1\}$. Employing h-refinement and p-refinement procedures in IGA, the desired mesh can be constructed from this coarse mesh. To study the convergence of the numerical approach, meshes with 16, 64, 256 and 1024 elements (see Figure 18) and with different order of NURBS (from quadratic to quintic) are investigated. The results are given in Table 5 which shows finer the mesh or higher the NURBS order, more accurate the results, as expected. The L2 error norm for the plate deflection is plotted in Figure 19 which shows sub-optimal convergence for quadratic NURBS, almost optimal convergence for cubic NURBS and super-optimal convergence for quartic and quantic NURBS is obtained using the Lagrange multiplier method. The IGA solution and the absolute error distribution for cubic NURBS with 64 elements are also presented in Figure 20.

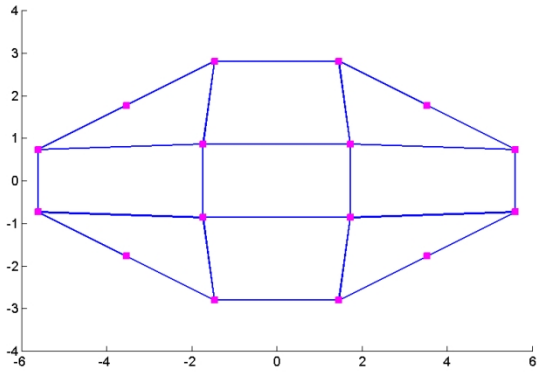

(a)

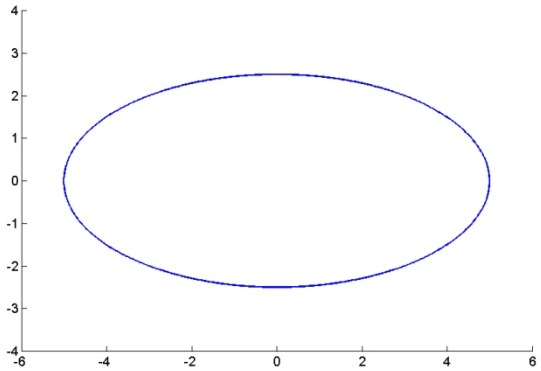

(b)

Figure 17. Initial discretized geometry: (a) control mesh; (b) physical mesh

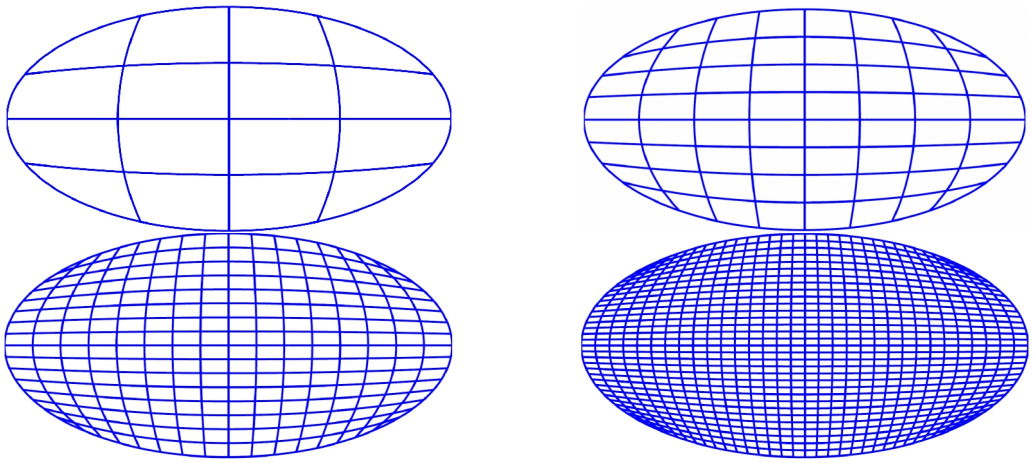

Figure 18. Physical meshes with 16, 64, 256 and 1024 elements for the elliptical plate

Table 5. Dimensionless central deflection of CCCC elliptical plate under uniform load

Num. of Elements	Order of NURBS basis function				Exact Solution (Equation 4.8)
	2	3	4	5	
16	8.7314	10.6106	10.5941	10.5934	10.5932
64	10.0775	10.5948	10.5932	10.5932	
256	10.4654	10.5933	10.5932	10.5932	
1024	10.5613	10.5932	10.5932	10.5932	

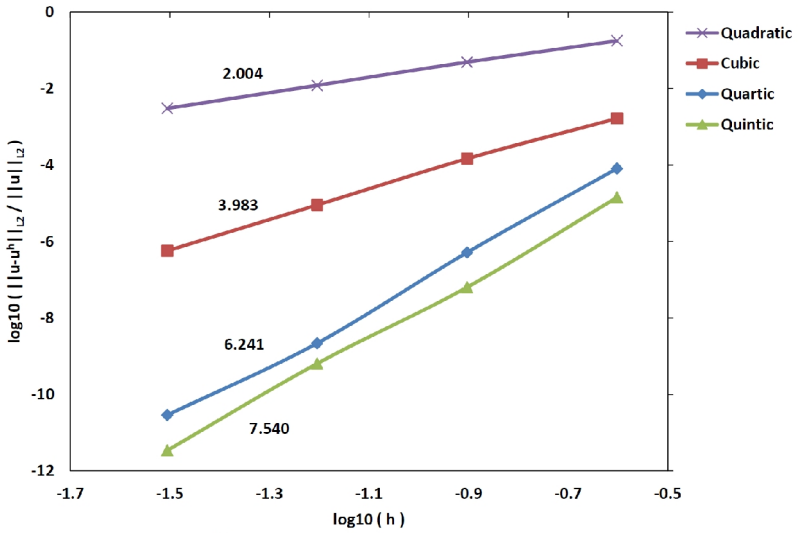

Figure 19. Comparison of L^2 error norm for different order of NURBS basis functions

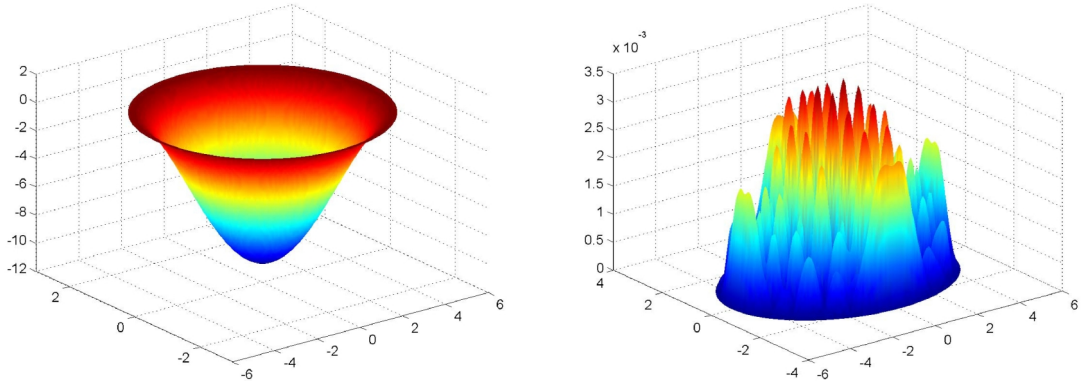

Figure 20. Isogeometric solution for cubic NURBS basis function with 64 elements based on the Lagrange multiplier method (Left) and the absolute error (Right)

5. Concluding remarks

In this paper, an efficient technique based on the Lagrange multiplier method is suggested for imposition of essential boundary conditions in NURBS-based isogeometric analysis. In this approach, the Lagrange multipliers are defined on a set of physical boundary points. In general, these interpolation points are Griville abscissas on the essential boundary. Among the various possible choices of the interpolation space for the Lagrange multipliers, the Lagrange shape functions have been adopted. The results of several simulations have illustrated that excellent solution accuracy and rate of convergence are obtained by applying

this approach. It also offers a far higher rate of convergence where it is compared with the direct imposition of essential boundary condition.

Acknowledgements

The financial support of Iran National Science Foundation (INSF) is gratefully acknowledged.

References

[1] T.J.R. Hughes, J.A. Cottrell, Y. Bazilevs, Isogeometric analysis: CAD, finite elements, NURBS, exact geometry and mesh refinement, *Computer Methods in Applied Mechanics and Engineering*, Vol. 194, 39-41 (2005) 4135-4195.

[2] Y. Bazilevs, T.J.R. Hughes, NURBS-based isogeometric analysis for the computation of flows about rotating components, *Computational Mechanics*, Vol. 43, 1 (2008) 143-150.

[3] Y, Bazilevs, V.M. Calo, T.J.R. Hughes, Y. Zhang, Isogeometric fluid–structure interaction: theory, algorithms and computations, *Computational Mechanics*, Vol. 43, 1 (2008) 3-37.

[4] D.J. Benson, Y. Bazilevs, M.C. Hsu, T.J.R. Hughes, Isogeometric shell analysis: the Reissner–Mindlin shell, *Computer Methods in Applied Mechanics and Engineering*, Vol. 199, 5-8 (2010) 276-289.

[5] W.A. Wall, M.A. Frenzel, C. Cyron, Isogeometric structural shape optimization, *Computer Methods in Applied Mechanics and Engineering*, Vol. 197, 33-40 (2008) 2976-2988.

[6] T. Belytschko, Y.Y. Lu, L. Gu, Element free Galerkin methods, *International Journal for Numerical Methods in Engineering*, Vol. 37, 2 (1994) 229-256.

[7] W.K. Liu, S. Jun, Y.F. Zhang, Reproducing kernel particle methods, *International Journal for Numerical Methods in Fluids*, Vol. 20, 8-9 (1995) 1081-1106.

[8] J. Bonet, S. Kulasegaram, Correction and stabilization of smooth particle hydrodynamics methods with applications in metal forming simulations, *International Journal for Numerical Methods in Engineering*, Vol. 47, 6 (2000) 1189-1214.

[9] S. Fernández-Méndez, A. Huerta, Imposing essential boundary conditions in mesh-free methods, *Computer Methods in Applied Mechanics and Engineering*, Vol. 193, 12-14 (2004) 1257-1275.

[10] T. Zhu, S.N. Atluri, A modified collocation method and a penalty formulation for enforcing the essential boundary conditions in the element free Galerkin method, *Computational Mechanics*, Vol. 21, 3 (1998) 211-222.

[11] M. Griebel, M.A. Schweitzer, A particle-partition of unity method. Part V: Boundary conditions, in S. Hildebrandt, H. Karcher (Eds.), *Geometric Analysis and Nonlinear Partial Differential Equations*, Berlin: Springer-Verlag, 2002, pp. 517-540.

[12] I. Babuska, U. Banerjee, J.E. Osborn, Meshless and generalized finite element methods: A survey of some major results, in M. Griebel, M.A. Schweitzer (Eds.), *Meshfree Methods for Partial Differential Equations*, International workshop, Universität Bonn, Germany, September 11-14, 2001, Lecture Notes in Computational Science and Engineering, Vol. 26, Berlin: Springer-Verlag, 2002, pp. 1-20.

[13] T. Belytschko, D. Organ, Y. Krongauz, A coupled finite element–element-free Galerkin method, *Computational Mechanics*, Vol. 17, 3 (1995) 186-195.

[14] A. Huerta, S. Fernández-Méndez, Enrichment and coupling of the finite element and meshless methods, *International Journal for Numerical Methods in Engineering*, Vol. 48, 11 (2000) 1615-1636.

[15] A. Embar, J. Dolbow, I. Harari, Imposing Dirichlet boundary conditions with Nitsche's method and spline-based finite elements, *International Journal for Numerical Methods in Engineering*, Vol. 83, 7 (2010) 877-898.

[16] D. Wang, J. Xuan, An improved NURBS-based isogeometric analysis with enhanced treatment of essential boundary conditions, *Computer Methods in Applied Mechanics and Engineering*, Vol. 199, 37-40 (2010) 2425–2436.

[17] P. Costantini, C. Manni, F. Pelosi, M. Lucia Sampoli, Quasi-interpolation in isogeometric analysis based on generalized B-splines, *Computer Aided Geometric Design*, 27 (2010) 656-668.

[18] L. Piegl, W. Tiller, *The NURBS book*, New York: Springer-Verlag, 1997.

[19] G.R.Liu, *Mesh free methods: moving beyond the finite element method*, USA: CRC, Boca Raton, 2003.

[20] J. Hoschek, D. Lasser, *Fundamentals of computer aided geometric design*, Massachusetts: A.K. Peters, Ltd. Wellesley, 1993.

[21] I. Babuska, The finite element method with Lagrange multipliers, *Numerische Mathematik*, Vol. 20, 3 (1973) 179-192.

[22] F. Brezzi, On the existence, uniqueness and approximation of saddle-point problems arising from Lagrangian multipliers, Rev. Franç Automatique Inform Rech Opér, *Ser Rouge Anal Numér*, Vol. 8, 2 (1974) 129-151.

[23] S.P. Timoshenko, J.N. Goodier, *Theory of Elasticity*, 3rd ed., New York: McGraw Hill, 1970.

[24] S.P. Timoshenko, S. Woinowsky-Krieger, *Theory of Plates and Shells*. 2nd ed., New York: McGraw-Hill, 1959.

[25] E. Ventsel, T. Krauthammer, *Thin Plates and Shells: Theory, Analysis and Applications*, 1st ed., New York: CRC Press, 2001.

[26] S. Shojaee, E. Izadpanah, A. Haeri, Imposition of essential boundary conditions in isogeometric analysis using the Lagrange multiplier method, *International Journal of Optimization in Civil Engineering*, Vol. 2, 2 (2012) 247-271.